Parametric Simulation of Nonlinear Shear Key Behavior on the Seismic Response on Bridge Abutments

By B.V. Fell[1] and M.W. Salveson[2]

Abstract

The effects of a phenomenological non-linear model for transverse bridge abutment shear keys on the dynamic response of a typical reinforced concrete bridge are investigated. The dynamic response of bridge structures modeled with a fully linear model, based on the current California Department of Transportation (Caltrans) Seismic Design Criteria (SDC), are compared to analysis results which incorporate a non-linear ductile model for the transverse abutment shear key. Various bridge geometries are considered to determine which common design parameters affect the accuracy of the current linear models used in design. In each case, the linear and non-linear models are subject to a suite of 80 ground acceleration time histories and the maximum lateral bent deformations are compared. The results suggest that the linear model currently used in analysis and design of California bridges is, in general, conservative across a wide range of configurations and fundamental periods of vibration (0.5s – 1.4s). Column displacements from the nonlinear model are as much as 43% larger than predicted displacements from the linear model. However, the study highlights a possible deficiency of the current modeling approach for highly flexible bridges.

[1] Assistant Professor, Dept of Civil Engineering, California State University, Sacramento, Sacramento, CA
[2] Assistant Professor, Dept of Civil Engineering, California State University, Sacramento, Sacramento, CA

INTRODUCTION

During an earthquake event, the behavior of reinforced concrete bridge abutments is commonly governed by the stiffness and strength of transverse shear-keys and longitudinal soil conditions. While the effect of bent strength and ductility capacity has long been the focus of the research community (Aschheim et al., 1997, Lehman and Moehle, 1998, 2004), a somewhat recent thrust has been on bridge end conditions, including the effects of the abutment and soil behavior (Romstad et al., 1995, Goel and Chopra, 1997, Shamsabadi et al., 2005, Huang et al., 2008) on the longitudinal stiffness and strength of the structure. These studies have provided the design community with accurate and practical models (e.g., Section 7 of the Caltrans Seismic Design Criteria) which consider complex end effects and substantially define the dynamic properties of the structure. The focus of this paper is on the influence of bridge end details on the lateral, or transverse, structural properties, which are governed by markedly different mechanisms as compared to the longitudinal behavior. The most apparent difference is the frequent lack of the soil resistance in the transverse direction and the reinforcing details of the abutment shear key, both of which contribute to substantially different stiffness and strength values.

Unlike the models developed for the longitudinal response of bridge end conditions, the Caltrans Seismic Design Criteria recommends simplified assumptions for the transverse abutment stiffnesses which have evolved through convenience and intuition, rather than the physical governing behavior. The current procedure utilizes a linear, elastic spring with half the stiffness of the adjacent bridge bent. The intent of this approach is to provide a suitable end boundary condition to suppress spurious (lateral twisting) modes of vibration that would result if the pinning effects of the abutment shear keys were neglected. However, considering the significance of the overall stiffness in the dynamic response of a structure and the resulting force and deformation distribution for each component, it is questionable whether this assumption should be an acceptable practice. While the current design methodology may be suitable for ordinary configurations, research has not verified the appropriateness of transverse stiffness recommendations made in the SDC. Moreover, the shear keys are viewed more as a brittle fuse during the seismic response of the structure, rather than a ductile, energy dissipating element. Thus, not only is there a need to investigate the stiffness and strength of shear keys, but there is also an opportunity to develop an energy dissipating element from the shear key response. The latter requires examining the nonlinear response of these elements designed with modern practices while also developing innovative reinforcement details to improve the ductility of the shear keys, but is not the focus of this paper.

Two models are investigated herein that describe the transverse response of the abutment shear key. The first model is a linear elastic spring with half the stiffness of the closest bent as specified by current design provisions. For comparison, a nonlinear spring is developed and employed which considers deck to shear key gap effects, an ultimate strength capacity, and inelastic deformation capacity. The elastic stiffness for the nonlinear spring is calculated with a two dimensional continuum model of a typical shear key cross-section while the ultimate strength is calculated by using code specified shear friction equations. Seven bridge configurations are selected to compare the effect of each model across a wide-range of parameters. A suite of ground motions is used to conduct dynamic analyses on each of the seven models using both the linear and nonlinear shear key model with varying strength capacities.

Key findings from the analyses are discussed with implications to the application of each model in the design of bridges.

The paper begins by introducing the motivation for the current study, including common geometries and loading on bridge abutment components. Next, the analytical modeling approach is presented along with the bridge archetype structures and associated ground motions for the dynamic analyses. Finally, the results are discussed in the context of current code-based modeling assumptions.

BACKGROUND AND MOTIVATION

Abutment shear keys, shown schematically in Figure 1, are typically designed as brittle elements, with the assumption that they will lose strength capacity during a large seismic event if the abutment is supported on piles, thus serving as a fuse that protects the piling. In the case of spread footing conditions, the keys are still considered brittle elements, albeit with a larger strength capacity so as to ensure they remain intact. For detailed information on the design procedures, the reader is referred to the current edition of the Caltrans Seismic Design Criteria which provides a complete set of guidelines for post-tensioned reinforced concrete bridges.

As an overview of the current seismic design procedure, the lateral earthquake design loads are dependent on an elastic acceleration demand (e.g., acceleration response spectrum curves found in Appendix B of the SDC). The acceleration demands are period dependent such that for periods larger than 0.2-0.4 seconds, spectral accelerations commonly decrease as the period increases. In considering the elastic stiffness of a typical bridge system, a large degree of uncertainty is associated with the abutment shear key behavior in the case of moderate to severe earthquake events. While the stiffness of the bridge bent and abutment stiffness in the longitudinal (normal) direction are considered less variable due to a large amount of research conducted on the subassembly (Aschheim et al., 1997, Lehman and Moehle, 1998, Lehman, and Moehle, 2004, Romstad et al., 1995, Goel and Chopra, 1997, Shamsabadi et al., 2005, Huang et al., 2008), the lateral (transverse) behavior of abutments have not been rigorously investigated. Thus, the current seismic design criterion assumes that the lateral abutment stiffness is 50% as stiff as the nearest bents (section 7.8.2 in the SDC). This assumption is driven by the fact that end conditions (typically a shear key) will soften considerably at the Maximum Considered Earthquake (MCE) level, while providing significant elastic rigidity during low and moderate level seismic events.

This assumption for the lateral abutment stiffness was introduced primarily as an analysis simplification, rather than basing the stiffness on the physical size and reinforcing details of the shear-key. The intent is to allow minimal transverse deformation at the abutments while suppressing spurious modes of vibration from an unsupported transverse end condition. Previously, informal design procedures included a two-part analysis with pinned and free boundary conditions, respectively, to capture the extreme conditions of the transverse end conditions. The bridge components would then be designed for the worst case of the two analysis results.

With these observations, there is a need to investigate the appropriate model for transverse abutment response for use in analysis and design. The current assumption based on the adjacent bent and bent stiffness warrants study and validation through comparison of a more realistic model of the expected behavior at the abutment. If invalid, an advancement of bridge design methodologies would be to incorporate a lateral stiffness model into the seismic design criterion for abutments, similar in form to the longitudinal model proposed by Romstad et al., (1995). Regardless of the accuracy of current seismic provisions, a nonlinear model of transverse shear key behavior would be valuable within a Performance Based Earthquake Engineering (PBEE, Deierlein et al., 2003) framework where accurate estimates of Engineering Demand Parameters (EDPs) such as inelastic deformation are a necessity.

Parametric Study of Bridge Geometries and Shear Key Strengths

Post-tensioned box girder bridges can be adapted to meet a wide variety of physical constraints. Thus, it is difficult to capture the wide-spectrum of behavior with the parametric study presented in this paper. Rather, the current investigation is meant to query key geometrical features that, when coupled with the boundary conditions at the abutments, may influence the overall response of the structure.

A 3-span bridge described in Table 1 (geometry A) and illustrated in Figures 2 and 3 was designed for a high seismic risk site in Riverside, California. For simplicity, the structure is considered to be on a horizontal and vertical tangent. Furthermore, the bridge is relatively short, such that modifications to the abutment boundary conditions are expected to have the greatest effect on the overall structural response. The substructure consists of two bents, each with two 1.2 m circular columns with cross-sectional properties shown in Figure 3a. The bridge deck is designed as a 1.6 m deep post-tensioned box girder illustrated in Figure 3b. The bent and deck details remain constant across each of the geometries described below. The longitudinal abutment springs assume an abutment backwall depth of 1.6 m, a width of 11.0 m, and a movement rating of 50 mm.

Six dissimilar bridge configurations (B, C, D, E, F and G) listed in Table 1 were included in the study, each representing a change to a key geometric feature or modeling parameter which may affect structural response. Configuration B modifies configuration A by rotating the bridge deck at a large (45 degree) skew to the bents and abutments. The effect of a large skew angle is expected to generate transverse loading at the abutments due to increased longitudinal inertia forces, and vice versa, resulting in higher mode effects. Configuration C is similar to configuration A with the exception of decreased end span lengths to 16.8 m. Such configurations, while not standard, are by no means uncommon and may change the dynamic response of the system. To study the effect of large deformations on shear-key response, configuration D provides an exceedingly flexible structure, relative to the original geometry of A, by doubling the length of each column. While configuration D may be very flexible compared to most bridges, the geometry was included to investigate the case of large period structures. Configuration E is identical to configuration A, except the bridge columns are assigned a fixed-fixed boundary condition, generating a lower period of vibration in the transverse direction. This is in contrast to bridges A-D which are pinned-fixed. While not provided herein, a strength check was done to ensure the increased shear demand resulting from the fixed-fixed condition remained less than the nominal capacity of the column. Finally, configurations F and G are identical to configuration A, except that the bent foundation soils are assumed to be compliant and are modeled with transverse and longitudinal springs.

Configuration F represents a relatively flexible soil-structure interaction, and configuration G represents a relatively stiff soil-structure interaction.

In addition to studying the effect of superstructure and substructure geometries, the ultimate strength of the shear-key was also included as a parameter. While the gap distance is relatively constant for a majority of bridges due to code provisions and practice, the shear key strength tends to be more variable, as it is driven by the magnitude of the resisting friction force from the steel reinforcing cage specified by the designer. An ultimate strength of 1054 kN is used as an upper-bound strength value along with 527 kN for the lower-bound. The larger capacity is calculated in the following section by assuming a shear-friction failure mode across a construction joint, while the latter is taken as half the original strength to investigate the sensitivity to this parameter. For most practical shear key geometries, the elastic stiffness of the key is quite large, so this parameter was not investigated in the parametric study.

ANALYTICAL MODEL DEVELOPMENT

DYNAMIC MODEL

The bridge geometries were modeled using a refined mesh of one-dimensional elements as shown in Figure 4. To isolate the effect of the shear-key model on the structural response, linear elastic frame and spring elements were used for the bridge superstructure and columns and abutment springs, respectively. The spring elements at the abutment are consistent with the requirements of the SDC Section 7.8.1, "*Longitudinal Abutment Response*". The shear key elements were modeled with springs orthogonal to the longitudinal abutment spring and assigned properties consistent with the requirement of the SDC, Section 7.8.2, "*Transverse Abutment*

Response" (i.e., half the stiffness of the adjacent bent), or the non-linear model described in the following section. The effects of compliant soils at foundations were considered for bridge configurations E and F. For other bridge configurations, the foundation supports at the bents were assumed to be rigid. Torsional restraint was not provided at the bridge abutments. Additional model parameters, such as superstructure and substructure section and material properties, were set in compliance with all applicable SDC recommendations and requirements and are summarized in Table 1.

In common design practice, linear bridge analyses for seismic loading conditions are performed through a modal superposition approach such that the elastic mode shapes and participation factors amplify the modal deformation response from a site specific acceleration spectrum. While efficient and suitable to quantify maximum force and deformation demands on the structure, modal superposition is restricted to linear behavior and neglects record-to-record variability. Thus, for both the linear and non-linear shear-key model, seismic effects are assessed through dynamic time history analyses such that the analytic model is solved at each time step employing the (unconditionally stable) Newmark constant average acceleration time integration technique.

While the mass and stiffness matrices are accurately calculated from known material parameters and bridge geometries, the formulation of the damping matrix is somewhat more intangible. For this study, the damping matrix is constructed directly through a mass-proportional approach such that a 5% of critical damping ratio is achieved at the first mode of vibration.

CONSTITUTIVE MODELS

Standard constitutive models, consistent with the current edition of the Caltrans SDC, are used such that gross cross-section properties are assumed for the post-tensioned superstructure and cracked section properties are assumed for the substructure column bents. The modulus of elasticity for all concrete elements is calculated using the concrete compressive strength according to $E_c = 57{,}000\sqrt{f_c'}$.

For the non-linear shear-key model, a rate-independent force-deformation model is assumed for each of the two shear keys at each abutment shown in Figure 4. The formulation of the model illustrated in Figure 5 includes an initial gap distance of 25 mm between the bridge superstructure and the shear key, followed by a linear-elastic response and a perfectly plastic region to represent the post failure behavior of the key. While the gap distance will change as the shear key fuses and deforms plastically, the ultimate shear key force and shear key stiffness are assumed to remain unchanged throughout the analysis.

The shear key strength capacity, F_{key}, is determined from the shear friction method ($F_{key} = \mu A_s F_y$), where A_s is the cross sectional area of the reinforcing steel in the shear key failure plane, μ is the static coefficient of friction, and F_y is the yield strength of steel (414 MPa). The value of μ depends on the construction details, where monolithic construction will provide a larger friction coefficient as compared to a cross-section with construction joints. For this work, μ is taken to be 1.0. Figure 6a illustrates the cross-section of the shear key, where A_s = 2550 mm^2, producing a capacity of 1054 kN. Adjusting the coefficient of friction to 0.5 - a conservative value for a concrete to concrete interface with construction joints - yields a shear key strength of

527 kN. Both strength values (1054 and 527 kN) will be used in the parametric study to investigate the influence of strength on the overall bridge performance.

The stiffness of the shear key for the nonlinear model is calculated with a plane stress, two-dimensional continuum model illustrated in Figure 6b. The material properties are assumed isotropic with a homogenous elastic modulus equal to 28,600 MPa. Referring to Figure 6b, the key is fixed along the bottom surface and loaded in the lateral direction with a pressure load distributed over the approximate height of the superstructure. The nodal reactions at the base, divided by the average deformation over the height of the superstructure generates a stiffness of 18,900 kN/mm. Relative to the stiffness of the bents, this large value creates the effect of having a pinned end condition once the transverse gap has closed.

Soil-Structure Interaction

Soil springs are used to model compliant foundation soils for bridge configurations F and G. Lateral soil springs at bent foundations are typically estimated by examining the lateral stiffnesses of the various soil layers at the bridge site and analyzing the interaction between the structural pile and the surrounding soil. In particular, the p-y method, as adopted by the U.S. Department of Transportation in 1984 and subsequently by most of the State Highway Departments, is applied for this work with the use of a popular commercial software package. The method is based on the work by Matlock (1970), Reese (1975), Welch and Reese (1972), and Nyman (1980).

For this work, two separate foundations were considered to envelope the response due to flexible and stiff foundation-to-soil conditions. Each column in Configuration F is assumed to be supported by twelve 1.2m-long, steel HP310x79 (HP12x53) piles with an axial service capacity of 41 metric tons. The pile cap is assumed to be free, while the soil is assumed to be layered gravel, sand and silt. The configuration yields a lateral pile stiffness of approximately 1.75 kN/mm. Pile group effects are neglected, and the total lateral stiffness of each column footing is assumed to be 21 kN/mm. Alternatively, the lateral stiffness of each column footing for configuration G is obtained by assuming the substructure is constructed with cast-in-place drilled piles to represent a stiffer foundation condition. Each column in Configuration G is assumed to be supported by twelve cast-in-drilled-hole 610 mm diameter concrete piles with an axial service capacity of 64 metric tons). The pile cap is assumed to be fixed against rotation, while the soil is layered silty sand and sandy clay. The configuration yields a lateral pile stiffness of approximately 14 kN/mm. Pile group effects are neglected, and the total lateral stiffness of each column footing is assumed to be 168 kN/mm.

To model the effect of compliant soil, a linear-elastic spring was placed in the longitudinal and transverse direction at the base of each column.

Ground Motion Selection

The ground motions used for the time history analyses are adapted from a database of broad-band ground motions produced for the Pacific Earthquake Engineer Research (PEER) Center Transportation Research Program (TRP). For the TRP study, 40 pairs of orthogonal motions were chosen for relatively generic bridge structures, and sites with M = 7, R = 10 km and soil-type with an average shear wave velocity of 250 m/s in the upper 30 m soil strata (Jayaram and Baker, 2010). To characterize the expected seismic demands at the site, the ground motions are scaled to the Maximum Considered Earthquake (MCE) level using the 5%-damped spectral acceleration for each structure at the transverse period of vibration or first mode if a pure transverse mode was not applicable (Vamvatsikos and Cornell, 2002). While this type of scaling has been shown to create somewhat biased analysis results (Luco and Bazzurro, 2007 and Baker, 2011), for the purposes of this comparative work on the shear-key influence, the ground motion scaling is not rigorously considered.

Figure 7c and 7d illustrates the acceleration response spectra for the scaled Fault Parallel (FP) motions for the transverse mode period of vibration of structures E and A, respectively. The darker line on each figure corresponds to the site-specific acceleration demands while the dashed line represents the mean of the scaled ground motions. An eigenvalue analysis demonstrated that, for structures A, C and E, the first and second modes correspond to the longitudinal and transverse mode of deformation, respectively. Due to the skewed geometry of Bridge B, the first mode (T = 1.42 seconds) was a mixed longitudinal-transverse mode. For structure D (long column), the first mode shape represents a torsional motion while the transverse deformation is represented at a higher mode.

RESULTS AND DISCUSSION

The twenty-one bridge models, consisting of seven geometrical and constitutive variations with two shear key strength values for the nonlinear transverse shear key model, and the standard linear elastic representation, were analyzed for 40 pairs of ground motions. Thus, for each of the seven bridge configurations, results from 80 ground motions applied to the linear elastic model are compared to results from nonlinear models with the same ground motion loading of varying shear-key strength capacities. For the purposes of this study, the maximum combined deformation in the lateral and longitudinal directions of each bent is reported. To compare a single quantity across each structure, the deformations are combined with the square-root-sum-square (SRSS) rule, where, typically, the lateral direction controls the magnitude of the SRSS deformation.

The results from the comparative analyses are shown in Tables 2 and 3, and Figures 8 and 9. Referring to the table, the geometric mean, coefficient of variations (COV), and median maximum combined column deformations are listed in the table for each of the seven bridge configurations and the three shear key representations (one linear and two non-linear). The deformations from the two nonlinear shear key models are normalized by the linear elastic deformation for each ground motion. Figures 8a-d plot the ratio of the maximum deformation from the nonlinear shear key models to the maximum deformation from the linear model for both shear key strengths as a function of the spectral acceleration at the scaled mode of vibration for each of the 80 ground motions. In general, the results in Figure 8 illustrate the unscaled ground motion intensity (S_a (T, 5%) has little effect on the comparison between the linear and nonlinear deformations. Figure 9 demonstrates the influence of soil-structure interaction on the comparison between models. Note, the ground motions correspond to the Fault Normal and Fault Parallel direction as presented in Jayaram and Baker (2010).

Effect of Ultimate Shear Key Strength

Table 2 and Figure 8 demonstrate that the shear key strength has little effect on the median deformation demands across bridge geometries A, B, C, and E and a marginal effect for geometry D. For example, the median deformations for bridge A with a key strength of 1054 kN and 527 kN are 10.6 cm and 11.7 cm (equivalent drift of approximately 0.015 radians), respectively. Owing to the ductility demands of a weaker nonlinear shear key model, the models with a stronger key showed a smaller variation across the 80 ground motions.

Effect of Bridge Geometry

In general, the analysis results of the seven bridge configurations suggest that the current elastic shear key model predicts larger and more conservative deformations as compared to the use of a nonlinear representation of the key. The largest discrepancy between the results from the linear and nonlinear shear key models occurs for the archetype bridge structure, A. Referring to Table 2, the median maximum deformations recorded from the linear analyses are approximately 0.73 and 0.79 times smaller than the deformations for the nonlinear model with nearly pinned end conditions. Furthermore, Figure 8 demonstrates the significant dispersion of maximum deformations for both shear key strengths across the 80 ground motions for structures A and C-G. Structure B (skewed geometry), had the least scatter with a coefficient of variation of 0.09 and 0.10 for the two key strengths.

The least conservative results were generated by the analysis of the long column bridge (D) where the median maximum deformations recorded from the nonlinear analyses with nearly pinned end conditions are approximately 0.96 and 1.02 times the deformations for the linear model. However, referring to Figure 8d, structure D also had the largest standard deviation of the five analyses. Most likely, this result is due to the flexibility of the structure and the torsional nature of the fundamental mode of vibration. When comparing results through the square root of the sum squares of the transverse and lateral deformations, a more torsional mode of deformation may produce varying results across the 80 ground motions. Thus, the accuracy of the linear shear key model with respect to the nonlinear model for structure D may be more out of coincidence, rather than a truth from the study.

The analyses from structure E demonstrate that the linear model is most accurate for stiff, regular bridge geometries due to the effect of column stiffness on the transverse key stiffness in the linear model used in current California provisions (i.e., 0.5*k). An increase in bent stiffness generates a stiffer model for the key and approaches the true stiffness represented by the nonlinear model. From Table 2, the ratios between the analysis results are 0.93 and 0.96 for the different key strengths with coefficients of variation of 19 and 24%, respectively.

Effect of Linear and Nonlinear Shear Key Model

For configurations A, B, and C, the maximum deformations from the linear analyses are conservatively larger than the deformations from the nonlinear model, with the ratio $\Delta_{nonlinear}/\Delta_{linear}$ ranging from 0.73 to 0.86 across the two strength values. As discussed previously, the comparison of models on structure D (long column) appears to be accurate, but with a larger dispersion. The least scatter was recorded from the analysis results on bridge configuration B with the larger skew angle. A stiff, short period structure with regular geometry (configuration E), appears to be the most applicable use of the current provisions. The nonlinear shear key models consistently produce smaller deformations as compared to the linear model due to the pinning effect of the large stiffness calculated from the finite element model (Figure 6).

Effect of Soil Springs at Bents

For configurations F and G, and referring to Table 1, the soil springs at the bottom of the columns produce a structure with longer natural periods and associated deformations. Table 3 lists the results for configurations F and G with a compliant soil model and should be compared to configuration A in Table 2. For configuration F with relatively compliant soils, column deformations are 6% larger when compared to a configuration with a rigid base (configuration A). For configuration G with a stiff soil model, the results are approximately equal to those listed in Table 2 for configuration A. In both cases, the use of soil springs at the bases of the columns does not appear to have a significant effect on the comparison between the results obtained from the dissimilar modeling approaches of the shear key.

Summary

While several investigations have examined the longitudinal stiffness of bridge abutments there has not been a rigorous study on the lateral abutment stiffness and the effect on structural behavior during earthquake loading. Goel and Chopra (1997) reported field data from the instrumented US 101/Painter Street Overpass and partly investigated this stiffness; however, only two ground motions are discussed and only one produced significant inelastic response.

Perhaps due to the erstwhile lack of an analytical study, the current modeling assumptions for the transverse behavior of shear key elements in California developed primarily from convenience and assumed behavior. Assuming linear elastic behavior, the transverse abutment is represented with a spring boundary condition equal to half the stiffness of the adjacent bent. The likely reason for this is to reduce spurious modes of vibration, which may result from a free end condition, while accounting for the gap distance between the deck and shear key face. Furthermore, once the gap distance is closed, the stiffness of the transverse key is much larger than the assumed stiffness, so maximum deformations are likely to be conservatively large.

This paper presented a comparative study of the linear elastic shear key model suggested by California seismic provisions to a nonlinear representation, including a gap distance and inelastic deformation capacity. Mean and median maximum deformations on the bridge columns are recorded from 80 time history analyses using earthquake ground motions scaled to the Maximum Considered Earthquake (MCE) level for a site in Riverside, California. To investigate the sensitivity of the shear key models, a parametric study is presented using seven bridge configurations and two ultimate strength values for the nonlinear shear key model.

The results suggest that for relatively short and stiff bridges, the linear model is an accurate assumption and yields deformations which are marginally smaller than deformations recorded using a nonlinear model. Furthermore, considering the large stiffness value of the nonlinear shear key, a pinned assumption may be a suitable lateral boundary condition at the abutments for most bridge geometries. For more flexible, yet standard, bridge geometries (T > 1.0 seconds), the results suggest the current modeling approach may be overly conservative. The large standard deviation associated with the analysis results from a structure with long columns indicates that the current modeling approach may be, on average, unconservative for bridges with highly flexible substructures. Finally, while the nonlinear shear key model was developed in accordance with expected physical behavior, the true behavior of the shear key element may warrant future experimental work.

NOMENCLATURE

A_s	-	Area of steel reinforcement, mm^2
E_c	-	Elastic modulus of concrete, MPa
F_y	-	Yield strength of steel, MPa
M	-	Earthquake magnitude
R	-	Source to site distance, km
a	-	Nodal relative acceleration vector, m/s^2
a_g	-	Ground acceleration vector, m/s^2
c	-	Damping matrix, kg/s
$f_s(u)$	-	Nonlinear spring force response, kN
f'_c	-	Ultimate strength of concrete, MPa
k	-	Stiffness matrix, kN/m
m	-	Lumped nodal mass matrix, kg
u	-	Nodal relative displacement vector, m
v	-	Nodal relative velocity vector, m/s
Δ_{linear}	-	Maximum column deformation from linear shear-key model, cm
$\Delta_{nonlinear}$	-	Maximum column deformation from nonlinear shear-key model, cm
μ	-	Static coefficient of friction

Acknowledgements

The authors appreciate the input and review of California Department of Transportation Office of Earthquake Engineering. The assistance of Dokken Engineering in providing the archetype bridge geometry (labeled as A in the paper) is also acknowledged.

References

Aschheim, M.A., Moehle, J.P., Mahin, S.A. (1997). "Design and evaluation of reinforced concrete bridges for seismic resistance." Earthquake Engineering Research Center, University of California, Berkeley, 1997-03.

Baker, J.W. (2011). "Conditional Mean Spectrum: Tool for ground motion selection," Journal of Structural Engineering, ASCE, 137(3), 322-331.

Caltrans Seismic Design Criteria (SDC) Version 1.6, Caltrans. (2010).

Cornell, C.A. and Krawinkler, H. (2000). "Progress and Challenges in Seismic Performance Assessment," PEER Center News, 3(2).

Deierlein, G.G., Krawinkler, H. and Cornell, C.A. (2003). "A framework for performance-based earthquake engineering." Proceedings, 2003 Pacific Conference on Earthquake Engineering, Christchurch, New Zealand.

Goel, R.K. and Chopra, A.K. (1997). "Evaluation of bridge abutment capacity and stiffness during earthquakes." Earthquake Spectra, 13(1), 1-23.

Huang, J., Shield, C.K. and French, C.E. (2008). "Parametric study of concrete integral abutment bridges." Journal of Bridge Engineering, ASCE, 13(5), 511-526.

Jayaram, N., and Baker, J. W. (2010). "Ground-Motion Selection for PEER Transportation Research Program." Proceedings, 7th International Conference on Urban Earthquake

Engineering (7CUEE) & 5th International Conference on Earthquake Engineering (5ICEE), Tokyo, Japan.

Lehman, D.E., and Moehle, J.P. (1998). "Seismic performance of well confined concrete columns." Pacific Earthquake Engineering Research Center, Berkeley, CA. UCB/PEER 1998/01.

Lehman, D.E., and Moehle, J.P. (2004). "Experimental Evaluation of the Seismic Performance of Reinforced Concrete Bridge Columns." Journal of Structural Engineering, ASCE, 130(6), 869-879.

Luco, N. and Bazzurro, P. (2007). "Does amplitude scaling of ground motion records result in biased nonlinear structural drift responses?" Earthquake Engineering and Structural Dynamics, 36(13), 1813-1835.

Matlock, H.. (1970). "Correlations for Design of Laterally-Loaded Piles in Soft Clay." Paper No. OTC 1204, Proceedings, Second Annual Offshore Technology Conference, Houston, Texas, Vol. 1, 577-594.

Nyman, K. J., (1980). "Field Load Tests of Instrumented Drilled Shafts in Coral Limestone", Unpublished Masters Thesis, The University of Texas at Austin, May 1980.

Reese, L.C., Cox, W.R. and Koop, F.D. (1975). "Field Testing and Analysis of Laterally Loaded Piles in Stiff Clay." Paper No. OTC 2313, Proceedings, 7th Offshore Technology Conference, Houston, Texas, 1975.

Romstad, K., Kutter, B., Maroney, B., Vanderbilt, E., Griggs, M. and Chai, Y.H. (1995). "Experimental measurements of bridge abutment behavior." Report No. UCD-STR-95-1, Department of Civil and Environmental Engineering, University of California, Davis.

Shamsabadi, A., Ashour, M. and Norris, G. (2005). "Bridge abutment nonlinear force-displacement-capacity prediction for seismic design." Journal of Geotechnical and Geoenvironmental Engineering, ASCE, 131(2), 151-161.

Vamvatsikos, D. and Cornell, A.C. (2002). "Incremental dynamic analysis." Earthquake Engineering and Structural Dynamics, 31(3), 491-514.

Welch, R.C. and Reese, L.C. (1972). "Laterally Loaded Behavior of Drilled Shafts." Research Report No. 3-5-65-89, conducted for Texas Highway Department and U.S. Department of Transportation, Federal Highway Administration, Bureau of Public Roads, by Center for Highway Research, The University of Texas at Austin, May, 1972.

TABLES

Table 1 –Bridge properties

	A	B*	C	D	E	F	G
Periods of Vibration							
Mode 1 (sec)	1.31	1.42#	1.22	1.44#	0.74	1.54	1.34
Transverse (sec)	1.05#	n/a	1.00#	n/a	0.55#	1.26#	1.08#
SUPERSTRUCTURE							
No. of Spans	3						
Length (m)	97.5		73.2	97.5			
Superstructure depth (m)	1.6						
Span 1 Length (m)	29.0		16.8	29.0			
Span 2 Length (m)	39.6						
Span 3 Length (m)	29.0		16.8	29.0			
Strong Axis I (m^4)	93.0						
Weak Axis I (m^4)	2.39						
Cross-Sectional Area (m^2)	6.39						
Concrete Strength (f'_c, MPa)	27.6						
SUBSTRUCTURE							
Columns per Bent	2						
Column Diameter (m)	1.2						
Bent 2 Height (m)	6.1			12.2	6.1		
Bent 3 Height (m)	9.1			18.3	9.1		
Effective I (m^4)	0.0414						
Cross-Sectional Area (m^2)	1.16						
Concrete Strength (f'_c, MPa)	34.5						
Soil spring stiffness (kN/mm/pile)	n/a (fixed support)					1.75	14.0
SHEAR KEY							
Linear model							
Transverse stiffness – Abutment 1 (kN/mm)	15.4			1.92	61.6	15.4	
Transverse stiffness – Abutment 4 (kN/mm)	4.56			0.57	18.2	4.56	
Longitudinal Abutment Stiffness (kN/mm)	2.36						
Nonlinear model							
Gap distance (mm)	25						
Key stiffness (kN/mm)	18,900 kN/mm						
Ultimate strength (kN)	1054 & 527						

*Pier and abutments skewed 45° to deck

#Period used to scale ground motions

Table 2 – Maximum combined (SRSS) column deformation (cm) and ratio of maximum deformation from nonlinear and linear shear key analyses ($\Delta_{nonlinear}/\Delta_{linear}$) for fixed-base bridges.

Geometry	Shear-key Model	Strength (kN)	Mean	COV	Median
A	Nonlinear	1054	11.0	0.24	10.6
		527	12.2	0.31	11.7
	Linear	--	15.6	0.31	15.2
	$\Delta_{nonlinear}/\Delta_{linear}$	1054	**0.74**	**0.28**	**0.73**
		527	**0.81**	**0.26**	**0.79**
B	Nonlinear	1054	13.4	0.29	12.6
		527	13.9	0.31	13.1
	Linear	--	16.2	0.31	15.0
	$\Delta_{nonlinear}/\Delta_{linear}$	1054	**0.84**	**0.09**	**0.84**
		527	**0.87**	**0.10**	**0.86**
C	Nonlinear	1054	9.3	0.30	8.7
		527	9.7	0.34	9.0
	Linear	--	12.5	0.28	11.9
	$\Delta_{nonlinear}/\Delta_{linear}$	1054	**0.77**	**0.28**	**0.77**
		527	**0.80**	**0.22**	**0.79**
D	Nonlinear	1054	15.5	0.41	14.0
		527	18.3	0.58	14.8
	Linear	--	14.9	0.26	14.8
	$\Delta_{nonlinear}/\Delta_{linear}$	1054	**1.07**	**0.37**	**0.96**
		527	**1.22**	**0.44**	**1.02**
E	Nonlinear	1054	6.1	0.34	5.7
		527	6.6	0.35	6.5
	Linear	--	7.0	0.42	6.1
	$\Delta_{nonlinear}/\Delta_{linear}$	1054	**0.92**	**0.19**	**0.93**
		527	**0.99**	**0.24**	**0.96**

Table 3 – Maximum column deformation (cm) and ratio of maximum deformation from nonlinear and linear shear key analyses ($\Delta_{nonlinear}/\Delta_{linear}$) for flexible-base (deformable soil) structures.

Geometry	Shear-key Model	Strength (kN)	Mean	COV	Median
F (K_{soil} = 21 kN/mm)	Nonlinear	1054	11.8	0.28	11.2
		527	13.1	0.35	12.4
	Linear	--	14.8	0.33	13.3
	$\Delta_{nonlinear}/\Delta_{linear}$	1054	**0.84**	**0.25**	**0.86**
		527	**0.91**	**0.23**	**0.90**
G (K_{soil} = 168 kN/mm)	Nonlinear	1054	11.1	0.25	10.4
		527	12.4	0.30	11.8
	Linear	--	15.4	0.31	14.9
	$\Delta_{nonlinear}/\Delta_{linear}$	1054	**0.76**	**0.27**	**0.74**
		527	**0.84**	**0.26**	**0.81**

Figure 1

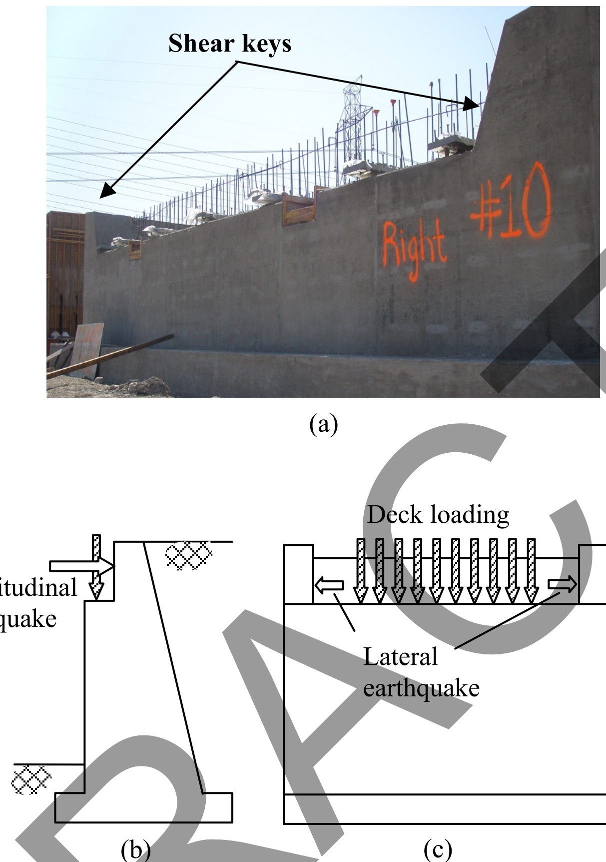

Figure 1 – (a) Abutment shear keys, (b) typical longitudinal and (c) lateral (transverse) abutment and shear key details and loading.

Figure 2

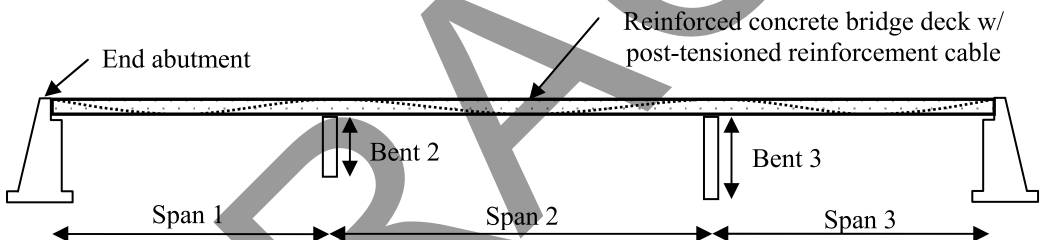

Figure 2 – Longitudinal elevation view of bridge geometry

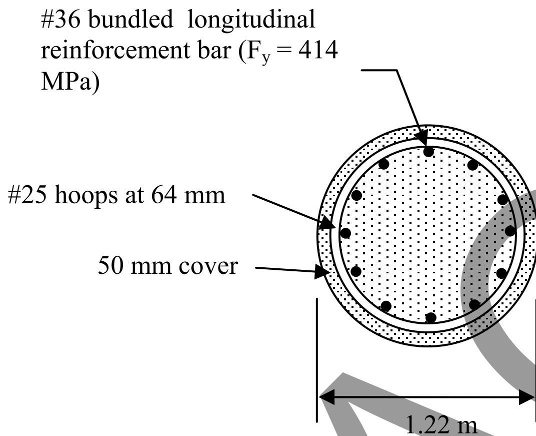

(a)

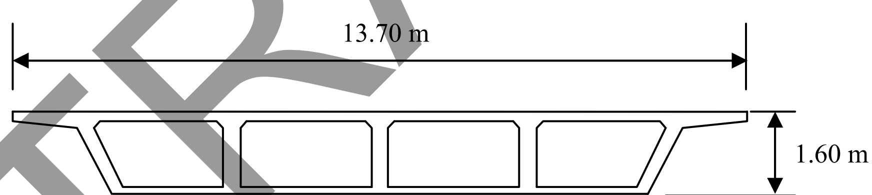

(b)

Figure 3 – (a) Typical column and (b) Bridge deck cross-sections.

Figure 4

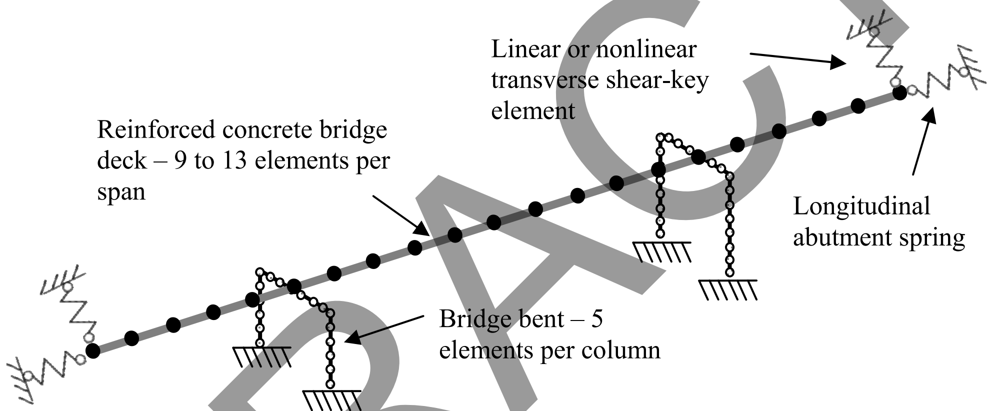

Figure 4 – Schematic analysis model and mesh for bridge geometry "A"

Figure 5

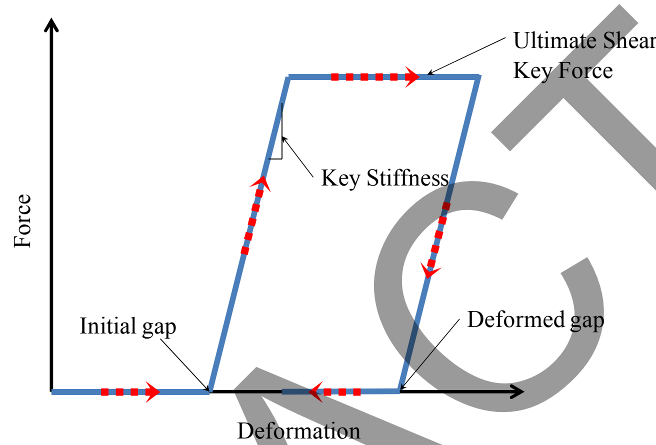

Figure 5 – Nonlinear shear key constitutive model

Figure 6

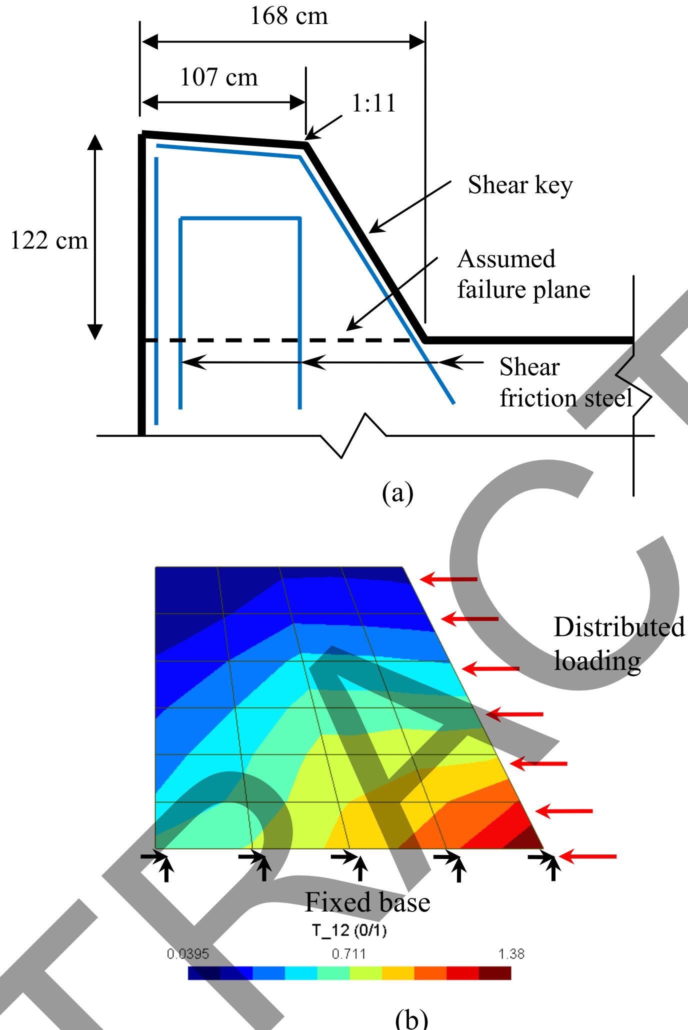

Figure 6 – (a) Detail/elevation and (b) Plane stress finite element model for abutment shear keys

Figure 7

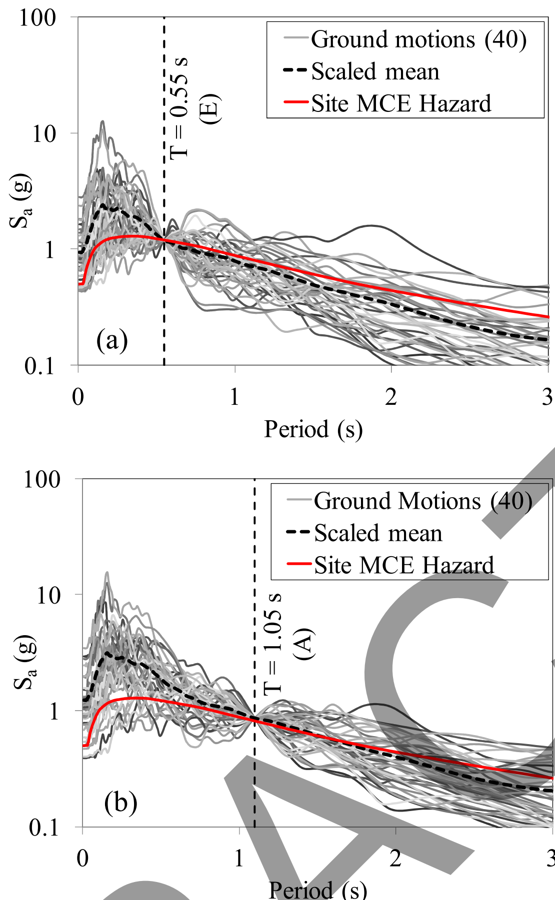

Figure 7 – Fault Parallel (FP) scaled ground motions at (a) 0.55 seconds for Bridge Structure E, and (b) 1.05 seconds for Bridge Structure A transverse mode periods.

Figure 8

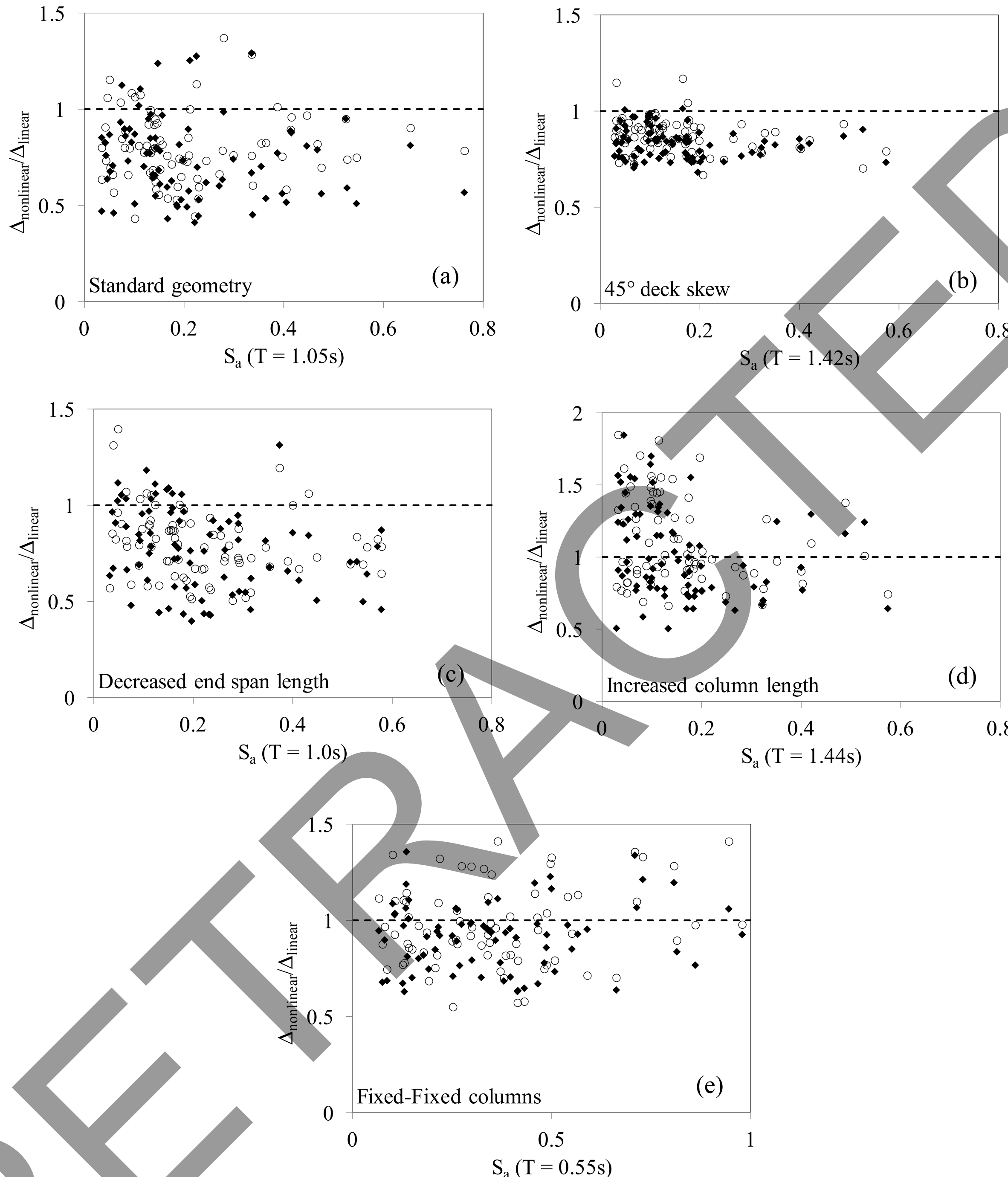

Figure 8 – Maximum column deformations from nonlinear shear-key model normalized by linear model deformations plotted versus the unscaled ground motion intensity for bridge configuration (a) A, (b) B, (c) C, (d) D, and (e) E (note the scale change). The plots also illustrate the effect of the two shear key strengths -- 1054 kN (♦) and 524 kN (o).

Figure 9

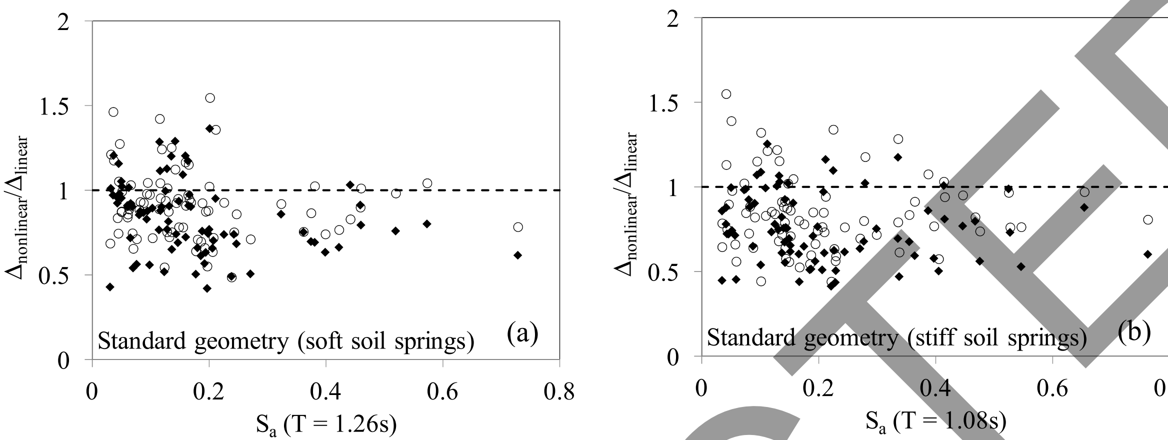

Figure 9 – Maximum column deformations from nonlinear shear-key model normalized by linear model deformations plotted versus the unscaled ground motion intensity for bridge configuration (a) F and (b) G with soil-structure interaction.

TABLES AND FIGURES CAPTIONS